Cellular & Molecular Immunology

ARTICLE

Induced regulatory T cells suppress Tc1 cells through TGF-β signaling to ameliorate STZ-induced type 1 diabetes mellitus

Li Zhou[1,2], Xuemin He[1], Peihong Cai[2], Ting Li[1], Rongdong Peng[1], Junlong Dang[2], Yue Li[1], Haicheng Li[1], Feng Huang[2], Guojun Shi[1], Chichu Xie[2], Yan Lu[2] and Yanming Chen[1]

Type 1 diabetes mellitus (T1D) is a chronic autoimmune condition in which the immune system destroys insulin-producing pancreatic β cells. In addition to well-established pathogenic effector T cells, regulatory T cells (Tregs) have also been shown to be defective in T1D. Thus, an increasing number of therapeutic approaches are being developed to target Tregs. However, the role and mechanisms of TGF-β-induced Tregs (iTregs) in T1D remain poorly understood. Here, using a streptozotocin (STZ)-induced preclinical T1D mouse model, we found that iTregs could ameliorate the development of T1D and preserve β cell function. The preventive effect was associated with the inhibition of type 1 cytotoxic T (Tc1) cell function and rebalancing the Treg/Tc1 cell ratio in recipients. Furthermore, we showed that the underlying mechanisms were due to the TGF-β-mediated combinatorial actions of mTOR and TCF1. In addition to the preventive role, the therapeutic effects of iTregs on the established STZ-T1D and nonobese diabetic (NOD) mouse models were tested, which revealed improved β cell function. Our findings therefore provide key new insights into the basic mechanisms involved in the therapeutic role of iTregs in T1D.

Keywords: type 1 diabetes mellitus; induced regulatory T cells; type 1 cytotoxic T cells; TGF-β; mTOR and TCF1

Cellular & Molecular Immunology (2021) 18:698–710; https://doi.org/10.1038/s41423-020-00623-2

INTRODUCTION

T1D occurs when pancreatic β cells cannot produce enough insulin to maintain normal blood glucose levels, and children are the main group that develop T1D. It has been reported that the prevalence of T1D in children is doubling approximately every 20 years in Europe,[1] and T1D currently causes an estimated loss of life expectancy of ~11–13 years.[2] Unfortunately, no therapeutic approaches can prevent or cure T1D,[3] and people with T1D need lifelong exogenous insulin therapy, which can only delay the progress of the disease. Thus, the development of new treatments that specifically target the pathogenesis of T1D and eventually prevent and cure T1D is urgently needed.

It is well recognized that β cell destruction is mainly mediated by autoimmunity. Signals generated by stressed, injured, or dying β cells recruit immune cells to the islets and activate these cells in the islets. Then, invading or resident macrophages and T cells release chemokines and cytokines in the islets and deliver proapoptotic signals to β cells, which ultimately destroy β cells.[4] $CD8^+$ T cells have been demonstrated to play a crucial role in this process. Papers have reported that in humans, $CD8^+$ cytotoxic T cells are the most abundant population during insulitis[5] and that islet-specific autoreactive $CD8^+$ T cells infiltrate the islets of individuals with recent-onset or longstanding T1D.[6] Tc1 cells (CD8-positive cells that secrete IFN-γ and TNF-α) mainly contribute to the cytotoxic activity of $CD8^+$ T cells in T1D, as Tc1 cells are more frequent in T1D patients than in normoglycemic people.[7] Furthermore, Tc1 cell adoptive transfer was shown to induce diabetes in nonirradiated adult rat insulin promoter-HA (RIP-HA) mice, while Tc2 cells (CD8-positive cells that secrete IL-4, IL-5, and IL-10) did not induce diabetes efficiently compared with Tc1 cells. Moreover, adoptive transfer of Tc1 cells from IFN-γ-deficient mice fails to induce diabetes in RIP-HA mice, suggesting that IFN-γ contributes to the pathogenic potential of cytotoxic Tc1 cells in T1D.[8]

Regulatory T cells (Tregs) are a class of suppressive T cells that can affect the function of $CD8^+$ T cells and are essential for inducing and maintaining immune tolerance. Tregs have deficiencies in frequency and/or function in T1D.[9–11] Furthermore, boosting Treg numbers (either by adoptive transfer or in vivo induction) has been found to be protective in animal and human T1D,[12–14] thus fueling interest in Tregs as a promising T1D immunotherapeutic target. Tregs are heterogeneous and can be divided into three populations: thymus-derived naturally occurring Tregs (nTregs), Tregs induced in vivo (pTreg), and Tregs induced ex vivo with IL-2 plus transforming growth factor-β (TGF-β) with or without retinoic acid or rapamycin (iTregs).[15] Among the three types of Tregs, nTregs are the most studied population in T1D treatment. Although work has been promising, there are several flaws that may significantly diminish the application of nTregs for T1D treatment, including (1) limited availability, (2) susceptibility to inflammation-induced apoptosis, (3) inability to suppress proinflammatory Th17 cells, and (4) self-conversion to effector T cells during inflammation.[16–18] In contrast, we and others have shown that iTregs do not have the flaws of nTregs

[1]Department of Endocrinology and Metabolism, Guangdong Provincial Key Laboratory of Diabetology, The Third Affiliated Hospital of Sun Yat-sen University, Guangzhou 510630 Guangdong, China and [2]Department of Clinical Immunology, The Third Affiliated Hospital of Sun Yat-sen University, Guangzhou 510630 Guangdong, China
Correspondence: Yan Lu (luyan36@mail.sysu.edu.cn) or Yanming Chen (chyanm@mail.sysu.edu.cn)

Received: 20 July 2020 Accepted: 10 December 2020
Published online: 14 January 2021

mentioned above[19–21] and maintain their suppressive function similar to nTregs. Moreover, iTregs have a better therapeutic effect than nTregs in autoimmune diseases, such as airway allergic inflammation,[18] rheumatoid arthritis,[22,23] and experimental allergic encephalomyelitis.[24] However, only a few studies have tested the role of iTregs in T1D,[25–27] and the underlying mechanism is still unclear. Here, we investigated the preventive and therapeutic roles of iTregs in T1D and further explored the impact of iTregs on IFN-γ production by Tc1 cells and the underlying mechanisms using an STZ-induced T1D model.

STZ can specifically induce β cell damage by binding to the receptor GLUT2 on pancreatic β cells. In contrast to a single high-dose STZ injection, which induces necrosis of β cells without lymphocyte infiltration, injection of multiple low doses of STZ can mimic T cell-mediated pancreatic injury.[28–31] Thus, we applied this well-established and broadly used STZ-T1D model[32–34] to test the role of iTregs during the progression of diabetes. We found that iTregs significantly ameliorated the progression of T1D by inhibiting Tc1 cells and rebalancing Treg/Tc1 cells in recipients. Furthermore, we showed that the suppressive effect of iTregs on IFN-γ production by Tc1 cells was due to the TGF-β-mediated combinatorial actions of mTOR and TCF1. Finally, we applied the established STZ-T1D and nonobese diabetic (NOD) mouse models to further confirm the improved β cell function observed after iTreg treatment. Thus, our data indicate that iTregs have great potential as a cell-based therapy for T1D.

MATERIALS AND METHODS

Mice

Wild-type C57BL/6 mice (male, 6–8 weeks old) were purchased from Guangdong Medical Laboratory Animal Center (Guangzhou, China). C57BL/6-FoxP3^{GFP} mice were generously provided by Dr. Talil Chatilla (University of Southern California, Los Angeles). C57BL/6 Thy1.1 transgenic mice were purchased from The Jackson Laboratory (Stock No: 000406). C57BL/6-FoxP3^{GFP} mice were backcrossed to B6 Thy1.1 mice, yielding Thy1.1$^+$ C57BL/6-FoxP3^{GFP} mice. Six-week-old NOD/ShiLtj mice were purchased from GemPharmatech (JiangSu, China), and ten-week-old NOD/ShiLtj mice were purchased from HuaFuKang Bio Company (Beijing, China). All animals were housed in the SPF animal facility in a temperature (72 ± 3 °F)- and air (50 ± 20% relative humidity)-controlled room with a 12-h light/dark cycle and were given a standard diet and tap water. All experiments using mice were performed in accordance with protocols approved by the Institutional Animal Care and Use Committee of Sun Yat-sen University.

Induction of diabetes

T1D was induced in Thy1.2$^+$ C57BL/6 mice (male, 6–8 weeks old) using multiple low-dose STZ (Sigma-Aldrich, St. Louis, MO, USA) injections. STZ was administered via the intraperitoneal route at a dose of 50 mg/kg in fresh cold 0.01 M citrate buffer (pH 4.5) within 20 min of dissolution for 5 consecutive days. Mice were fasted for 4–6 h prior to STZ injection, and 10% sucrose water was supplied overnight after the first injection to avoid sudden hypoglycemia.

Cell transfers and diabetes measurement

Naïve CD4$^+$ CD62L$^+$ T cells were MACS-sorted from the spleen or lymph nodes (the inguinal lymph nodes, mesenteric lymph nodes and axillary lymph nodes). In brief, the spleen or lymph nodes of Thy1.1$^+$ C57BL/6-FoxP3^{GFP} mice were collected, and single-cell suspensions were obtained by passing through a 40-μm cell strainer (352340, Corning, USA). Red blood cell lysis buffer (Sigma-Aldrich, St. Louis, MO, USA) was used to lyse splenic erythrocytes, and T cells were enriched using nylon wool (18369-50, Polysciences, USA). Then, the T cells were labeled with biotinylated anti-CD8 (100704, BioLegend), anti-B220 (103204, BioLegend), anti-CD11b (101204, BioLegend), anti-CD11c (117304, BioLegend), and anti-CD49b (103522, BioLegend) antibodies and anti-biotin microbeads (130-090-485, Miltenyi, Biotec, Germany). The cells were then subjected to depletion followed by positive selection after labeling with CD62L microbeads (130-049-701, Miltenyi Biotec, Germany) by an automatic magnetic cell sorter (MACS) (Miltenyi, Biotec, Germany). The purity of naïve CD4$^+$ CD62L$^+$ T cells was determined with flow cytometry, and naïve CD4$^+$ T cells with a purity >90% (please see Supplementary Fig. S1) were used for iTregs induction. iTregs were induced with recombinant human IL-2 (50 U/mL, R&D Systems) in the presence of recombinant human TGF-β (2 ng/mL, R&D Systems) or Med cells (CD4$^+$ Foxp3$^-$ cells) with only recombinant human IL-2 for 3 days. To determine intervention effects, 3.0×10^6 iTregs or Med cells suspended in 200 μl phosphate-buffered saline (PBS) were injected via the tail vein on the first day of STZ administration. In addition, STZ-induced model mice receiving 200 μl PBS were considered an additional control. Nonfasting blood glucose levels were monitored twice a week over the following 30 days using an Embrace One Touch blood glucometer (OMNIS Health, USA). Blood glucose concentrations exceeding 300 mg/dL or 16.7 mmol/L in two consecutive daily measurements were considered to indicate diabetes onset. Cages were changed every 3–4 days since mice developed symptoms of polyuria. For some experiments, an ALK5 inhibitor (Sigma-Aldrich) was given through i.p. injection at a dose of 0.5 mg per mouse on days 0, 7, 14, 21, and 28 to explore the role of TGF-β signaling in iTregs-mediated protection from T1D.

To determine the role of iTregs in established T1D, we made use of two models: STZ-T1D and NOD mice. For the STZ-T1D model, diabetes was induced in male C57BL/6 mice, and iTregs (3.0×10^6) induced from C57BL/6 mice under the conditions mentioned above were transferred into diabetic mice via the tail vein on day 7. The nonfasting blood glucose concentration was measured every other day within one week after cell transfer and 1–2 times per week thereafter. For some mice, we transferred the same dose of iTregs a second time on day 26, and blood glucose levels were monitored thereafter. For NOD mice, 3.0×10^6 iTregs induced in vitro from naïve CD4$^+$ T cells isolated from C57BL/6 mice were injected into 6-week-old and 10-week-old female mice via the tail vein. The nonfasting blood glucose concentration was measured 1–2 times per week. IPGTT and immunohistochemistry were performed to evaluate the function of β cells.

Histology and immunohistochemistry

Pancreas samples were fixed overnight in 10% formalin and embedded in paraffin. All embedding, sectioning, and H&E staining were performed by Servicebio Company (Wuhan, China). For assessment of insulin and glucagon production in the pancreas, two consecutive sections were stained with anti-insulin (1:1600, Abcam 63820) or anti-glucagon (1:8000, Abcam ab92517) antibodies, and the staining was visualized with anti-rabbit DAB-HRP (OMap) secondary antibodies; nuclei were counterstained with hematoxylin and a bluing reagent. Area measurement was performed with ImageJ software. For morphometric analysis of islet size and β cell area (positive insulin staining), each islet was traced and analyzed manually with ImageJ software. One section per pancreas in the preventive experiment (iTregs given at the same time of the STZ injection) and three sections per pancreas in the therapeutic experiment (iTregs given after diabetes onset) were used, and all islets seen on the sections were measured for analysis. Sections were evaluated by at least two different people to avoid subject bias. In brief, islets seen in pancreatic sections imaged at 200× magnification were captured with an Olympus microscope (Tokyo, Japan). For islet area measurement, the "Freehand selections" tool was used to draw the outline of islets in images with scale bars, and then the "measure" tool was used for area measurement. The size of islets is

reported in the Results section and expressed as μm^2. To quantify β cell area in relation to islet area, images were first converted to RGB stacks, and then the islet outline was drawn, followed by automatic thresholding. β cell area in relation to islet area could be read after using the "measure" tool.

Assessment of insulitis

Pancreatic tissue samples were stained with hematoxylin and eosin (H&E). The degree of insulitis was determined from three nonsequential slides from 3 to 5 individual mice. Every islet on each section was scored as previously described[35]: 0 = no lymphocytic infiltration; 1 = peri-insulitis (<30%); 2 = <50% islet infiltration; and 3 = >50% islet infiltration.

Enzyme-linked immunosorbent assay (ELISA)

Blood was collected from each mouse on day 15 after STZ injection and clotted at room temperature for 1 h, followed by incubation at 4 °C overnight. The serum was frozen at −80 °C until analysis. Serum insulin and C-peptide levels were measured by ELISA using a mouse C-peptide and insulin ELISA kit (Nanjing Herb Source Bio-Technology Co., Ltd, China) according to the manufacturer's instructions.

Intraperitoneal glucose tolerance test (IPGTT)

Glucose tolerance was evaluated using a conventional IPGTT conducted 15 days after STZ administration. Mice were given 20% glucose via i.p. injection at a dose of 2.0 g/kg body weight. Blood samples were collected at 0, 15, 30, 60, and 120 min via tail vein bleeding. Blood glucose levels were measured using a glucometer (OMNIS Health, USA).

Murine naïve $CD8^+$ T cell differentiation in vitro

Naïve $CD8^+$ $CD62L^+$ T cells were purified from the spleen or lymph nodes of $Thy1.2^+$ C57BL/6 mice via magnetic beads isolation (Miltenyi, Biotec, Germany) in the same way that naïve $CD4^+CD62L^+$ T cells were isolated. iTregs induced in vitro were cocultured with naïve $CD8^+$ $CD62L^+$ T cells (1:1) during in vitro differentiation. Naïve $CD8^+$ T cells were stimulated with anti-CD3 (1 μg/ml) and anti-CD28 (1 μg/ml) antibodies (both from BioLegend) in the presence of irradiated (30 cGy) syngeneic non–T cells (1:1) and recombinant mouse IL-12 (20 ng/ml, R&D Systems). After 3 days in culture, differentiated cells were restimulated with PMA and ionomycin (Sigma-Aldrich) for 5 h, with brefeldin A (BFA, BioLegend) added for the last 4 h. The expression of IFN-γ was then measured by flow cytometry. To determine the possible mechanisms, an ALK5 inhibitor (10 μM) was added to the coculture systems, and the cell differentiation ratio, mTOR activation and TCF1 expression were determined.

Flow cytometry analysis

Antibodies against CD4 (GK1.5, PerCP/Cy5.5), CD8 (53–6.7, PerCP/Cy5.5), Thy1.1 (OX-7, PE), Foxp3 (MF-14, Alexa Fluor 647), IFN-γ (XMG1.2, APC), IL-17 (TC11-18H10.1, PE), and Neuropilin-1 (3E12, PE) were purchased from BioLegend. An antibody against Foxp3 (FJK-16s, PE-Cyanine7) was purchased from Invitrogen. Antibodies specific for phospho-S6 ribosomal protein (Ser240/244) (D68F8, Alexa Fluor 647) and TCF1 (C63D9, Alexa Fluor 647) were purchased from Cell Signaling Technology. An Annexin V-FITC apoptosis detection kit (BMS500FI-300, Invitrogen) was used to evaluate cell apoptosis. Results were obtained on a BD FACSCalibur or BD LSRFortessa flow cytometer and analyzed using FlowJo. For ex vivo IFN-γ detection, lymphocytes were isolated from the spleen, mesenteric and inguinal lymph nodes (LNs) and pancreatic lymph nodes (PLNs) of diabetic mice on day 15 and day 30 after STZ injection and then stimulated in vitro with PMA (50 ng/ml) and ionomycin (500 ng/ml) for 5 h, with BFA added for the last 4 h. The intracellular expression of IFN-γ in $CD8^+$ T cells was analyzed by flow cytometry.

Quantitative polymerase chain reaction

Total RNA was isolated from the mesenteric lymph nodes and inguinal lymph nodes using the RNeasy Mini Kit (Qiagen, Valencia, CA, USA) according to the manufacturer's instructions; 1 μg RNA (OD260 nm/OD280 nm = 1.8–2.2) was used to synthesize first-strand cDNA using the Prime-Script RT Reagent Kit (Takara Bio Inc., Shiga, Japan). Quantitative polymerase chain reaction (qPCR) was performed on a 7500 Fast (ABI) RT-PCR instrument using SYBR Premix Ex Taq (Takara Bio Inc., Shiga, Japan). For qPCR, the following program was performed: 95 °C for 30 s (predenaturation); 95 °C for 5 s and 60 °C for 34 s for 40 cycles (amplification); 95 °C for 15 s, 60 °C for 1 min and 95 °C for 15 s (melt curve). The 2^ (-delta CT) method was used for calculations, and glyceraldehyde-3-phosphate dehydrogenase (GAPDH) was used as the housekeeping gene for normalization.

Western blots

Protein isolation from the mesenteric lymph nodes and inguinal lymph nodes was performed as previously described.[36] Western blotting was performed using the standard SDS-polyacrylamide gel electrophoresis method and enhanced chemiluminescence detection reagents (GE Healthcare Biosciences AB, Uppsala, Sweden). Antibodies against S6 ribosomal protein (S6), phospho-S6 ribosomal protein (Ser240/244) (pS6), TCF1 and GAPDH (all from Cell Signaling Technology, Beverly, MA) were used. Immunoreactivity was semiquantitatively measured by gel densitometric scanning and analyzed with an MCID image analysis system (Imaging Research, Inc.).

Statistical analysis

All results are presented as the mean ± standard deviation (s.d.). Differences among multiple groups were analyzed using one- or two-way analysis of variance (ANOVA). When ANOVA showed significant differences, pairwise comparisons between groups were performed with Dunnett's test. A two-tailed unpaired *t* test or the Mann-Whitney test was used for two-group comparisons. 1The chi-square test was used to compare diabetes incidence between groups. In all analyses, $P < 0.05$ was considered statistically significant.

RESULTS

iTregs ameliorated the progression of T1D and improved β cell function

To generate a T1D preclinical animal model, C57BL/6 mice were injected with multiple low doses of streptozotocin (STZ), a widely accepted model (Fig. 1A). Consistent with the data reported in the literature, STZ-injected mice exhibited progressive hyperglycemia 9 days after the first administration (Fig. 1B). To test the therapeutic potential of iTregs in T1D, C57BL/6 mice were adoptively transferred with 3×10^6 iTregs during the initial STZ injection. Notably, the mice infused with iTregs exhibited significantly decreased blood glucose levels compared with those in the STZ-treated only (Model) and $CD4^+$ $Foxp3^-$ cell infusion (Med) groups (Fig. 1B). Disease onset was markedly postponed following iTregs administration, and diabetes incidence was significantly decreased in the iTregs group compared to the control groups (Fig. 1C). To determine whether the improved glycemic control was associated with changes in β cells, we performed an intraperitoneal glucose tolerance test (IPGTT) on STZ-treated mice 15 days after iTreg administration. As shown in Fig. 1D, the blood glucose levels of mice from all three groups reached a peak 15 min after intraperitoneal glucose injection. However, the iTregs-treated mice exhibited dramatically faster clearance of the glucose load from the body than those in the Model and Med groups; the differences reached significance at 120 min (Fig. 1D). The area under the

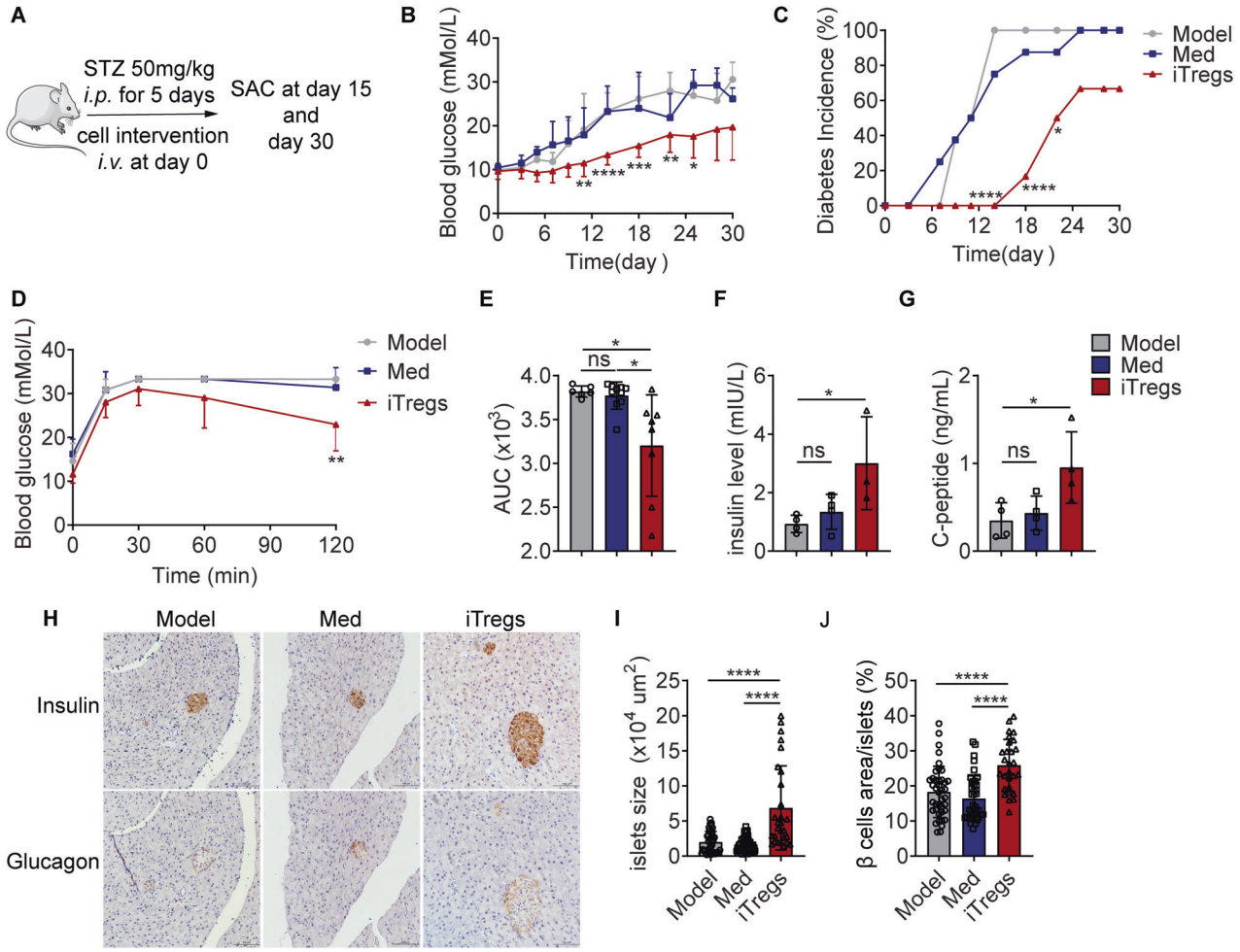

Fig. 1 iTregs ameliorated the progression of T1D and improved β cell function. iTregs ($CD4^+$ $Foxp3^+$) or Med cells ($CD4^+$ $Foxp3^-$) from $Thy1.1^+$ $FoxP3^{GFP}$ mice were injected into $Thy1.2^+$ T1D mice via the tail vein. **A** Schematic diagram for the in vivo experiment. **B** Nonfasting blood glucose levels of mice in the three groups ($n = 6$–8 per group). Two-way ANOVA; data are shown as the mean ± s.d. **C** Incidence of diabetes. The chi-square test was used to compare groups. **D** IPGTT results for day 15 after iTregs administration ($n = 6$–10 per group). The Mann–Whitney test was used to compare the Model and iTregs groups; data are shown as the mean ± s.d. **E** AUC for the IPGTT. Two-tailed unpaired *t* test; data are shown as the mean ± s.d. **F** and **G** Serum insulin and C-peptide levels on day 15 ($n = 4$ per group). Two-tailed unpaired *t*-test; data are shown as the mean ± s.d. **H** Representative images of insulin and glucagon staining. Insulin or glucagon expression is indicated by brown staining in cells. **I** and **J** All islets seen in one section per pancreas were used for analysis. Statistical analysis of islet size and β cell area in relation to islet area among the three groups ($n = 5$ per group). One-way ANOVA; data are presented as the mean ± s.d. Experiments were repeated three times. $^*P < 0.05$, $^{**}P < 0.01$, $^{***}P < 0.001$, and $^{****}P < 0.0001$; ns indicates no significance

curve (AUC) results derived from the IPGTT also proved that iTregs treatment could preserve β cell function (Fig. 1E). To further assess β cell function, serum insulin and C-peptide levels were tested on day 15. Consistent with the previous results, iTregs-treated mice showed increased insulin secretion and C-peptide production (Fig. 1F, G). To directly reveal the protective role of iTregs, histochemical analyses were performed to show the conservation of insulin-producing β cells (Fig. 1H). Taking all the islets as individual samples, iTregs-treated mice maintained a larger islet size (Fig. 1I) and exhibited significantly higher conservation of insulin-producing β cells per islet than those in the other two groups (Fig. 1J). If the average islet size or β cell area in relation to the islet area for each sample was used for analysis, we could see that the mice in the iTregs group still showed a larger islet size (Supplementary Fig. S2A) and more insulin-producing β cells per islet (Supplementary Fig. S2B). Taken together, these results demonstrate that iTregs can ameliorate the progression of T1D and protect β cell function in the STZ-induced T1D mouse model.

Adoptively transferred iTregs migrate to the pancreas and immune organs and maintain their phenotypic features in vivo

iTregs migration to diseased organs would be of great significance for therapeutic efficacy. To investigate the fate of adoptively transferred iTregs in vivo, iTregs derived from $Thy1.1^+$ $Foxp3^{GFP}$ reporter mice were transferred into $Thy1.2^+$ STZ-induced T1D mice, and the distribution of iTregs in different organs was examined by flow cytometry on days 15 and 30 postinjection. The results showed that injected iTregs ($CD4^+$ $Foxp3\text{-}GFP^+$) could be found in the spleen, lymph nodes (mesenteric lymph nodes and inguinal lymph nodes) and, importantly, PLNs on both day 15 and day 30 (Fig. 2A). Although the frequencies in the spleen and lymph nodes were decreased on day 30 regardless of whether gating on total live cells or $CD4^+$ T cells was used (Fig. 2B and C), the numbers of iTregs in these immune tissues remained stable (Fig. 2D). The frequency of iTregs among live PBMCs was almost the same on day 30 compared with day 15 but decreased when gated on total $CD4^+$ T cells (Fig. 2E–G). Most importantly and strikingly, iTregs migrated to the pancreas and persisted for at

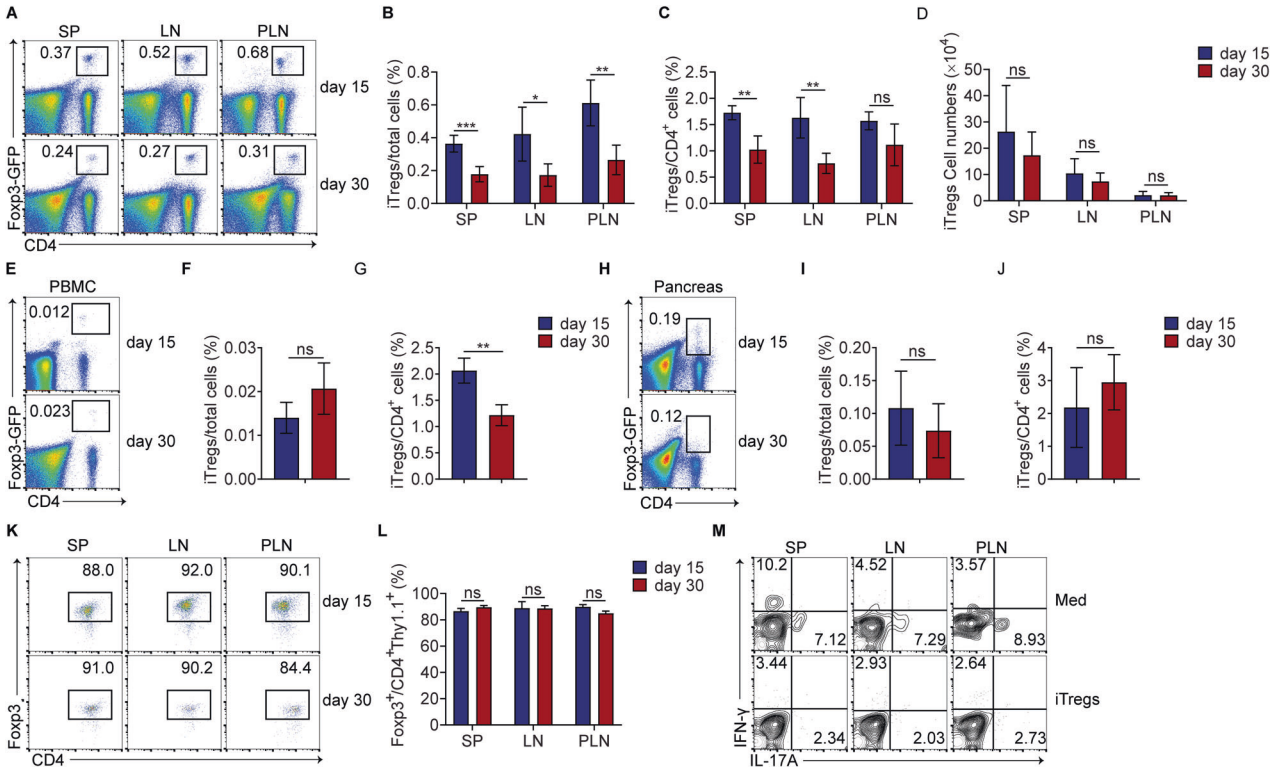

Fig. 2 Adoptively transferred iTregs migrate to the pancreas and immune organs and maintain their phenotypic features in vivo. iTregs ($CD4^+$ $Foxp3^+$) from $Thy1.1^+$ $FoxP3^{GFP}$ mice were injected into $Thy1.2^+$ T1D mice, and the iTregs organ distribution, engraftment and stability were then examined on day 15 and day 30. **A** Representative flow cytometry data showing the distributions of iTregs ($CD4^+$ GFP^+ cells) on day 15 (upper) and day 30 (lower) in the spleen (SP), mesenteric and inguinal lymph nodes (LNs) and pancreatic lymph nodes (PLNs). Gated on total live cells. Analysis of the iTregs cell percentage in the total live cells ($n = 5$) (**B**) and in relation to the $CD4^+$ T cells ($n = 5$) (**C**) in the SP, LNs and PLNs. Two-tailed unpaired *t*-test; data are shown as the mean ± s.d. **D** Analysis of iTregs cell numbers ($n = 7$) in the SP, LNs and PLNs. Two-tailed unpaired *t*-test; data are shown as the mean ± s.d. Representative flow cytometry data (**E**) and statistical data (**F**) showing the iTregs distribution in PBMCs gated on total live cells ($n = 5$). Two-tailed unpaired *t*-test; data are shown as the mean ± s.d. **G** Analysis of the iTregs cell percentage in relation to $CD4^+$ T cells ($n = 5$) in PBMCs. Two-tailed unpaired t-test; data are shown as the mean ± s.d. Representative flow cytometry data (**H**) and statistical data (**I**) showing the iTregs distribution in the pancreas gated on total live cells ($n = 5$). Two-tailed unpaired t-test; data are shown as the mean ± s.d. **J** Analysis of the iTregs cell percentage in the $CD4^+$ T cell population ($n = 5$) in the pancreas. Two-tailed unpaired t-test; data are shown as the mean ± s.d. Representative flow data (**K**) and statistical data (**L**) showing Foxp3 expression on day 15 and day 30 in cells in different tissues gated on $CD4^+$ $Thy1.1^+$ cells ($n = 3$). Two-way ANOVA; data are shown as the mean ± s.d. **M** Representative flow cytometry data showing the conversion of iTregs or Med cells into Th1 and Th17 cells on day 30; gated on $CD4^+$ $Thy1.1^+$ cells. Experiments were repeated three times. $^*P < 0.05$, $^{**}P < 0.01$, and $^{***}P < 0.001$; ns indicates no significance

least 30 days (Fig. 2H–J), indicating a strong ability to home to the target organ. To further investigate whether transferred iTregs could maintain their phenotypic features in vivo, we first examined the expression of Foxp3, the master transcription factor of regulatory T cells, which showed no changes between before (Supplementary Fig. S3) and after adoptive transfer (Fig. 2K, L). We next determined whether iTregs could convert into Th1 or Th17 cells under inflammatory conditions. Lymphocytes from the spleen, mesenteric lymph nodes, inguinal lymph nodes and pancreatic lymph nodes were harvested on day 30 postinjection and stimulated with PMA and ionomycin in vitro. IFN-γ and IL-17A production in iTregs was detected by intracellular staining. As shown in Fig. 2M, very few iTregs produced IFN-γ or IL-17A up to 30 days postinjection, whereas $Thy1.1^+$ $CD4^+$ $Foxp3^-$ cells from the Med group produced the above cytokines, indicating that iTregs did not convert into Th1 or Th17 cells in vivo.

iTregs rebalance endogenous IFN-γ-producing CD8 T cells and regulatory T cells in recipient STZ-induced T1D mice

To investigate the mechanism through which iTregs ameliorate the progression of T1D, we detected endogenous IFN-γ- and IL-17A-producing T cells and Tregs in recipient mice, as multiple lines of evidence show that the balance between effector T cells and Tregs is critical in T1D. The production of IFN-γ and IL-17A by endogenous $CD4^+$ or $CD8^+$ T cells ($Thy1.2^+$) from the spleen and lymph nodes (mesenteric, inguinal and pancreatic) of STZ-induced T1D mice was determined by intracellular staining after iTregs or control Med cells injection. Among the three groups (Model, Med, and iTregs), no differences were seen in the frequencies of IFN-γ- or IL-17A-producing $CD4^+$ T cells or IL-17A-producing $CD8^+$ T cells in the LNs (Supplementary Fig. S4), spleen, or PLNs (data not shown). However, the frequency of IFN-γ-producing $CD8^+$ T cells was significantly decreased in the iTregs group on both day 15 and day 30, indicating that iTregs might suppress the progression of T1D by inhibiting the IFN-γ-producing ability of $CD8^+$ T cells (Fig. 3A–C).

Next, we examined the effect of iTregs on endogenous Tregs, the frequency of which is decreased during T1D. As shown in Fig. 3D, E, the frequencies of endogenous Tregs ($Thy1.2^+$) in the spleen and lymph nodes (mesenteric, inguinal, and pancreatic) were significantly increased in iTregs-treated mice on day 15 compared to those in the Model and Med control groups, indicating that iTregs can improve the homeostasis of regulatory T cells. Neuropilin-1 (Nrp-1) can be used as a specific cell marker to distinguish nTregs from iTregs,[37] so we costained for Nrp-1 and Foxp3 to determine whether the increased population of

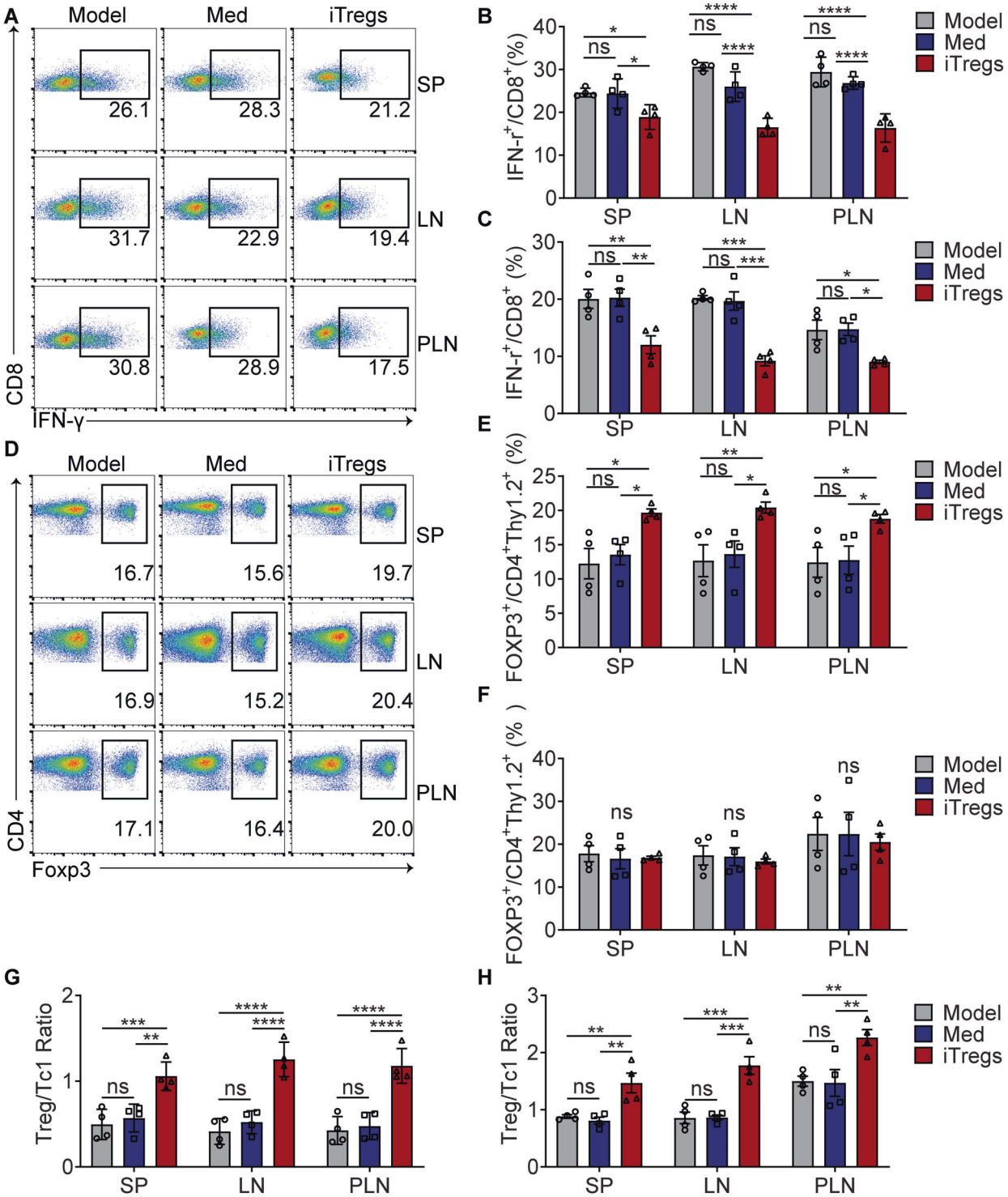

Fig. 3 iTregs rebalance endogenous IFN-γ-producing CD8 T cells and regulatory T cells (Tregs) in recipient STZ-induced T1D mice. Lymphocytes were isolated from the SP, LNs and PLNs and then stimulated in vitro with PMA (50 ng/ml) and ionomycin (500 ng/ml) for 5 h, with brefeldin A (10 μg/ml) added for the last 4 h, and the intracellular expression of IFN-γ on $CD8^+$ T cells was analyzed by flow cytometry. **A** Representative flow cytometry data showing IFN-γ expression gated on $CD8^+$ $Thy1.2^+$ T cells. Statistical analysis of the IFN-γ^+ population in $CD8^+$ $Thy1.2^+$ T cells on day 15 (**B**) and day 30 (**C**) in different tissues ($n = 4$). Two-way ANOVA; data are shown as the mean ± s.d. **D** Representative flow cytometry data showing the percentage of $Foxp3^+$ cells gated on $CD4^+$ $Thy1.2^+$ T cells on day 15. Statistical analysis of the $Foxp3^+$ cell population in $CD4^+$ $Thy1.2^+$ cells on day 15 (**E**) and day 30 (**F**) in different tissues ($n = 4$). Two-way ANOVA; data are shown as the mean ± s.d. Ratios of the recipient Treg percentage to the Tc1 percentage on day 15 (**G**) and day 30 (**H**) ($n = 4$ per group). Two-way ANOVA; data are shown as the mean ± s.d. $^*P < 0.05$, $^{**}P < 0.01$, $^{***}P < 0.001$, and $^{****}P < 0.0001$; ns indicates no significance

endogenous Tregs was primarily generated in the thymus (tTreg) or induced at peripheral sites (pTreg). As shown in Fig. S5, Nrp-1 expression on recipient Tregs was almost the same among the three groups, suggesting that iTregs mainly expanded endogenous nTregs, thus increasing the Tregs percentage in T1D mice. To confirm that iTregs can regulate the balance between endogenous regulatory T cells and IFN-γ-producing $CD8^+$ T cells (Tc1 cells), the Treg/Tc1 cell ratio was calculated. Although the frequencies of endogenous Tregs on day 30 were not elevated in iTreg-treated mice (Fig. 3F), the Treg/Tc1 cell ratio was significantly increased on both day 15 and day 30 in the iTregs group compared to the control groups (Fig. 3G, H). Thus, iTregs can rebalance Tregs and Tc1 cells in the T1D mouse model.

iTregs suppress Tc1 cells through TGF-β-dependent inhibition of mTOR signaling and promotion of TCF1 expression in vitro

To investigate the basis of the inhibition of IFN-γ-producing $CD8^+$ T cells by iTregs, we first examined the proliferative ability of $CD8^+$ T cells following iTregs administration by staining for Ki-67 and found that iTregs did not alter the proliferation of $CD8^+$ T cells (Fig. 4A, B). In addition, we did not observe different amounts of annexin V staining among the three groups, indicating that iTregs did not affect the apoptosis of $CD8^+$ T cells either (Fig. 4C, D). Then, we analyzed whether iTregs can inhibit Tc1 cell differentiation. As shown in Fig. 4E, iTregs significantly suppressed IFN-γ production during the in vitro polarization of Tc1 cells. Since the TGF-β signaling pathway has been suggested to modulate iTregs-mediated suppressive function,[38,39] we then examined whether TGF-β itself can also suppress Tc1 cell polarization and whether interfering with the TGF-β signaling pathway fails to inhibit IFN-γ production by $CD8^+$ T cells. Strikingly, TGF-β alone inhibited Tc1 cell differentiation, and moreover, the suppression of IFN-γ production by iTregs was completely abrogated when an inhibitor of activin-like kinase 5 (ALK5, also known as type 1 TGF-β receptor) was added to the in vitro coculture system (Fig. 4E, F), suggesting that the suppressive function of iTregs is dependent on TGF-β signaling.

Previous studies have shown that mTOR activity is required for $CD8^+$ T cells to maintain effector cell differentiation and function.[40–42] Thus, to determine whether iTregs suppress IFN-γ production by inhibiting mTOR signaling, we examined the phosphorylation of the S6 protein, an indicator of mTOR activation, in the Tc1 cell differentiation system with or without iTregs. We found that iTregs treatment led to a significant inhibition of S6 phosphorylation and this inhibition was partially dependent on TGF-β signaling, as the ALK5 inhibitor partially rescued the suppression of S6 phosphorylation (Fig. 4G, H).

Since T cell factor 1 (TCF1) is also involved in Tc1 cell differentiation, as inflammatory signals can inhibit TCF1 expression during $CD8^+$ T cell polarization and primed $CD8^+$ T cells lacking Tcf1 undergo default effector differentiation,[43–45] we evaluated TCF1 protein levels by flow cytometry to determine whether TCF1 is involved in the iTreg-mediated suppression of IFN-γ production in $CD8^+$ T cells. We found that TCF1 expression was indeed decreased during effector $CD8^+$ T cell differentiation, while iTregs treatment maintained high expression of the TCF1 protein, and this effect also partially relied on TGF-β (Fig. 4I, J). These results collectively suggest that the TGF-β-dependent inhibition of mTOR signaling and promotion of TCF1 are critical for the suppression of Tc1 cells by iTregs.

The therapeutic role of iTregs in STZ-induced T1D mice is dependent on TGF-β signaling

To extend our finding that TGF-β signaling is critical to the therapeutic role of iTregs in T1D, we investigated the effect of an ALK5 inhibitor on iTregs treatment. As described in Fig. 5A, the ALK5 inhibitor was injected five times at 1-week intervals in the context of the iTregs treatment protocol, as shown in Fig. 1A. Consistent with the in vitro results, disrupting TGF-β signaling with the ALK5 inhibitor abrogated the protective role of iTregs in STZ-induced T1D development, as suggested by elevated blood glucose levels (Fig. 5B) and an increased diabetes incidence (Fig. 5C). Moreover, the iTregs group showed a tendency toward amelioration of insulitis compared with the Model group, and the mice in the TGF-β signaling blockade group had more severe insulitis than those in the iTregs group (Fig. 5D-F). Decreases in islet size and β cell area in relation to islet area (Fig. 5D, G, H and Supplementary Fig. S6) further proved that the protective role of iTregs in STZ-T1D was dependent on TGF-β signaling. We further investigated whether mTOR signaling and TCF1 were involved in the effects of iTregs treatment, as suggested in vitro, and found that consistent with our in vitro data, mTOR mRNA and S6 phosphorylation levels were significantly suppressed, while TCF1 mRNA and protein expression was promoted and that inhibition of TGF-β signaling reversed these phenotypes (Fig. 5I–N). Taken together, these results suggested that the TGF-β-dependent inhibition of mTOR signaling and promotion of TCF1 were critical for the therapeutic effect of iTregs on the STZ-induced T1D mouse model.

iTregs improved β cell function in mice with established T1D

In addition to assessing the preventive role, we further evaluated the therapeutic effect of iTregs on established T1D using both STZ-T1D and NOD mice. A majority of mice developed diabetes on day 7 after the first STZ injection. These mice were randomly assigned to the iTregs-treated group or Model group. The working model is shown in Fig. 6A. As shown in Fig. 6B and C, six and two out of the ten mice in the iTregs-treated group had a nonfasting blood glucose level lower than 16.7 mmol/L 2 days and 4 days after cell intervention, respectively, while the mice in the Model group showed no relief of diabetes. Blood glucose levels rebounded to a level similar to that of the Model group 6 days after iTregs injection. The results of an IPGTT performed 1 week after cell transfer are shown in Fig. 6D. Although the blood glucose concentrations of all the mice treated with iTregs rebounded after 6 days, three mice still showed more powerful β cell function than the mice in the Model group, which contributed to the lower blood glucose level observed at 120 min during the IPGTT. The pancreas was isolated from these three mice for analysis one day after the IPGTT experiment to evaluate islet size and β cell function. All islets seen in three sections from each pancreas were evaluated for insulitis, islet area and β cell area in relation to islet area. Insulitis was scored from 0 to 3 based on the severity of infiltration. As shown in Fig. 6E–G, the severity of insulitis was markedly reduced 1 week after iTregs transfer. Taking all the islets as individual samples, iTregs-treated mice retained a significantly larger islet size (Fig. 6E and H) and had more insulin-producing β cells per islet than mice in the Model group (Fig. 6E and I). If the average islet size or β cell area in relation to islet area for each sample was used for analysis, we found that the mice in the iTregs group still had a larger islet size (Supplementary Fig. S7A), while the results for the β cell area in relation to the islet area did not reach statistical significance (Supplementary Fig. S7B). As the protective role for iTregs did not seem to be sustained for a long time, we reinjected 3×10^6 iTregs into the remaining mice 26 days after STZ injection. The blood glucose level did not decrease until 29 days after the second iTregs transfer, when one mouse out of seven showed a blood glucose level lower than 16.7 mmol/L (Fig. 6B).

We also evaluated the protective role of iTregs in NOD mice, which spontaneously develop T1D as a result of autoimmune-mediated destruction of pancreatic β cells. Although the difference in the blood glucose level between the two groups did not reach statistical significance (Supplementary Fig. S8A), iTregs remarkably slowed disease onset and decreased diabetes incidence (Fig. 6J). An IPGTT was also conducted to compare β cell

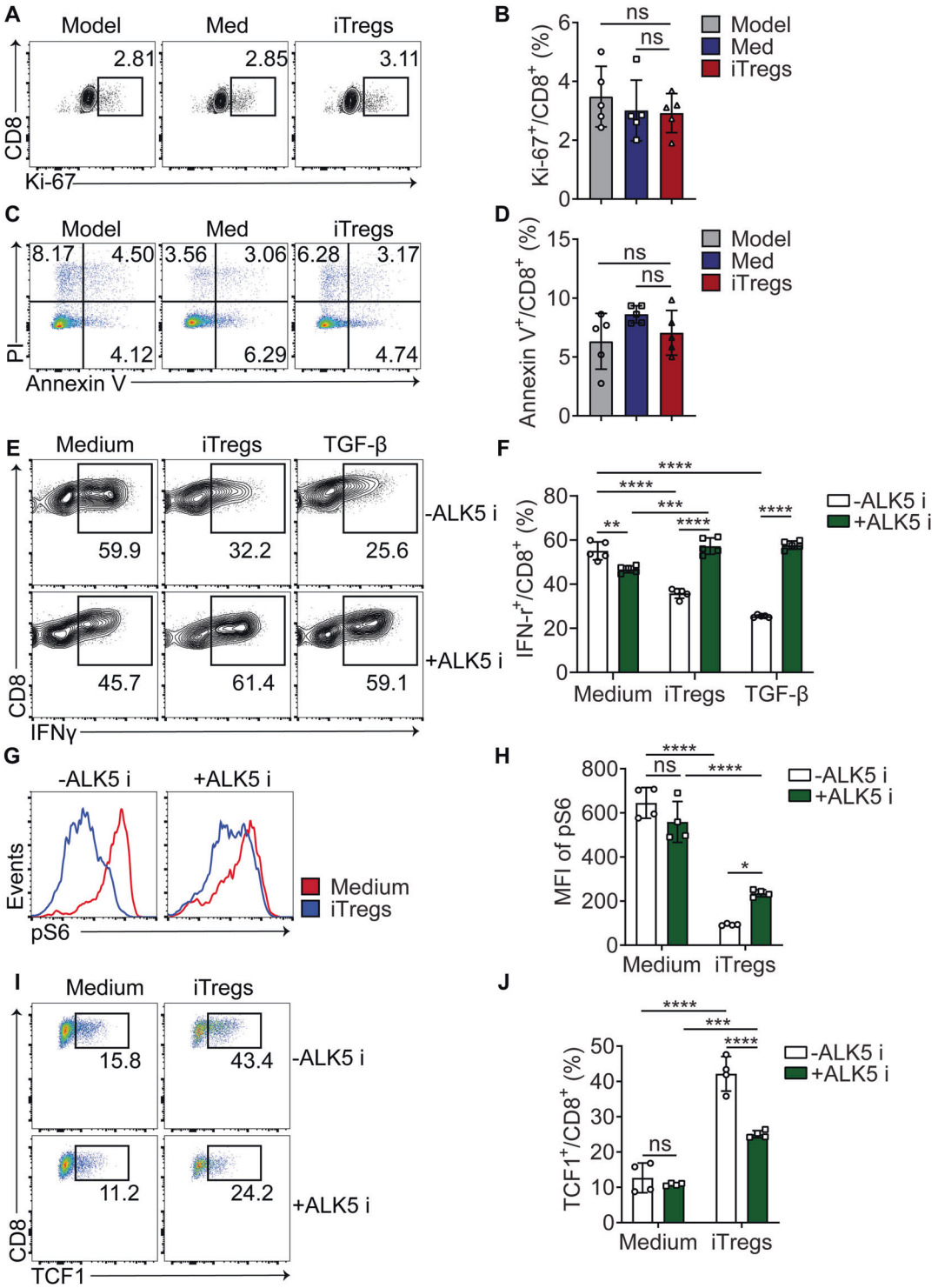

Fig. 4 iTregs suppress Tc1 cells through the TGF-β-dependent combinational action of mTOR and TCF1 signaling in vitro. Representative flow cytometry data and statistical analysis showed that iTregs did not affect $CD8^+$ T cell proliferation (**A**, **B**) or apoptosis (**C**, **D**) in vivo ($n = 5$). One-way ANOVA; data are shown as the mean ± s.d. Naïve $CD8^+$ T cells were polarized into Tc1 cells in vitro, and TGF-β (2 ng/ml), iTregs (iTregs: $CD8^+$ T cells = 1:1) or an ALK5 inhibitor (10 μM) was added to the culture system. **E**, **F** Representative flow cytometry data and statistical analysis showed that iTregs suppressed IFN-γ induction in $CD8^+$ T cells, similar to TGF-β, and this function relied on TGF-β signaling. Two-way ANOVA; data are presented as the mean ± s.d. of five independent experiments. **G**, **H** Representative flow cytometry data and statistical analysis showing the phosphorylation of the S6 protein at 24 hours among different groups. Two-way ANOVA; data are presented as the mean ± s.d. of four independent experiments. **I, J** Representative flow cytometry data and statistical analysis showed that iTregs maintained high expression of TCF1 at 72 h during Tc1 cell induction, and this effect was partially dependent on TGF-β signaling. Two-way ANOVA; data are presented as the mean ± s.d. of four independent experiments. *$P < 0.05$, **$P < 0.01$, ***$P < 0.001$, and ****$P < 0.0001$; ns indicates no significance

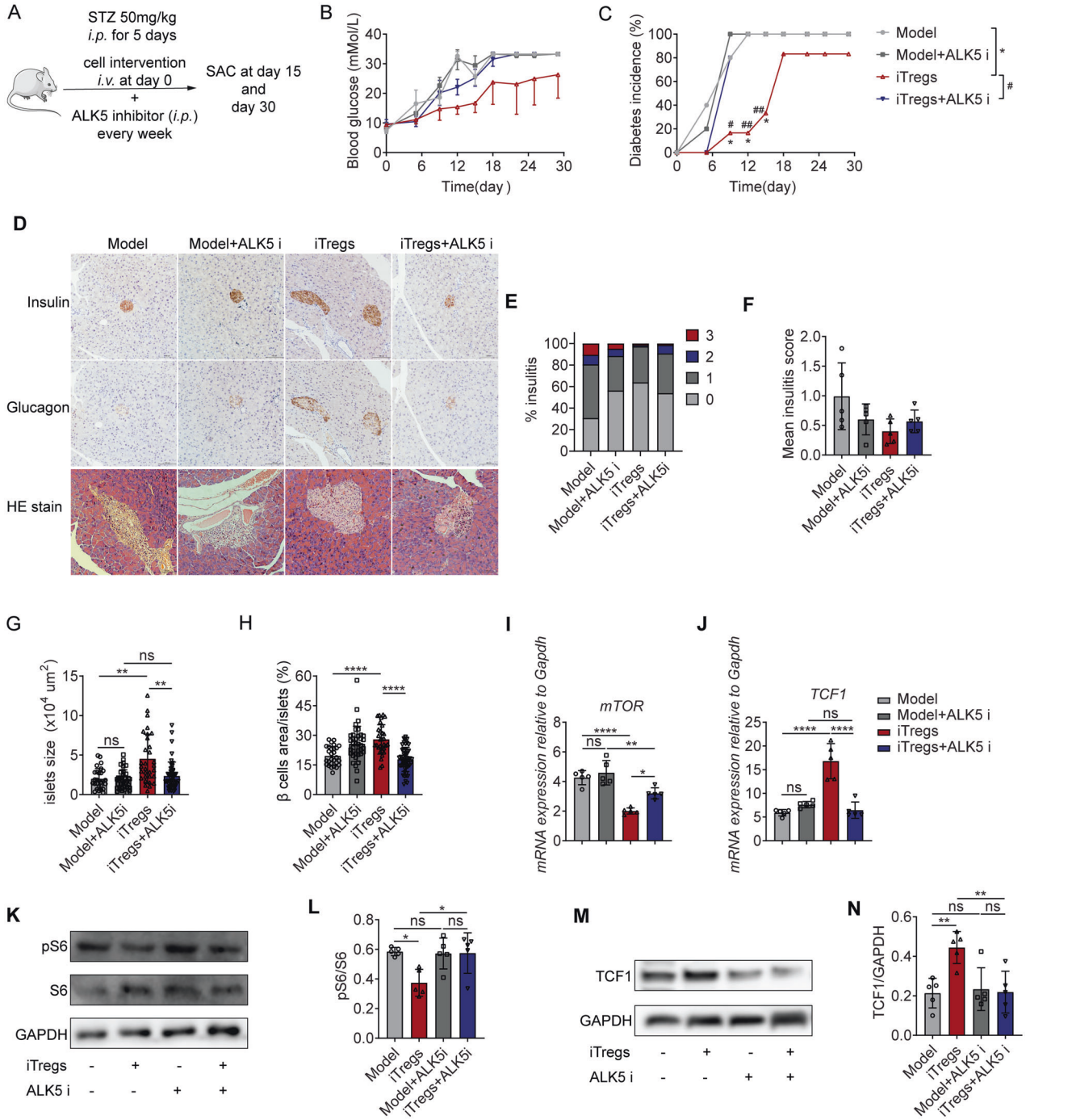

Fig. 5 The therapeutic role of iTregs in STZ-induced T1D mice is dependent on TGF-β signaling. An ALK5 inhibitor was injected into STZ-T1D mice to verify the role of TGF-β in iTregs-mediated protection. **A** Schematic diagram for the in vivo experiment. **B** Nonfasting blood glucose levels and diabetes incidence are shown ($n = 5$ for the Model group and $n = 6$ for the iTregs group). **C** Incidence of diabetes. Chi-square test comparing groups. **D** HE, insulin and glucagon staining in four groups. Insulin or glucagon expression is indicated by brown staining in cells. **E**, **F** Statistical analysis of insulitis scores among the four groups ($n = 5$ per group). One-way ANOVA; data are presented as the mean ± s.d. **G**, **H** All islets seen in one section per pancreas were used for analysis. Statistical analysis of islet size and β cell area in relation to islet area among the four groups ($n = 5$ per group). One-way ANOVA; data are presented as the mean ± s.d. **I**, **J** Relative mTOR and TCF1 mRNA levels in lymphocytes from the LNs on day 15 ($n = 5$ per group). One-way ANOVA; data are presented as the mean ± s.d. **K**, **L** Representative western blot and statistical analysis showing phosphorylated S6 protein expression in lymphocytes from the LNs on day 15 ($n = 5$ per group). One-way ANOVA; data are presented as the mean ± s.d. **M**, **N** Representative western blot and statistical analysis showing TCF1 protein expression in lymphocytes from the LNs on day 15 ($n = 5$ per group). One-way ANOVA; data are presented as the mean ± s.d. Experiments were repeated twice, with $n = 15$ for the Model, Model+ALK5 inhibitor, and iTreg+ALK5 inhibitor groups and $n = 16$ for the iTregs group in total. $^{*}P < 0.05$, $^{**}P < 0.01$, and $^{****}P < 0.0001$; ns indicates no significance

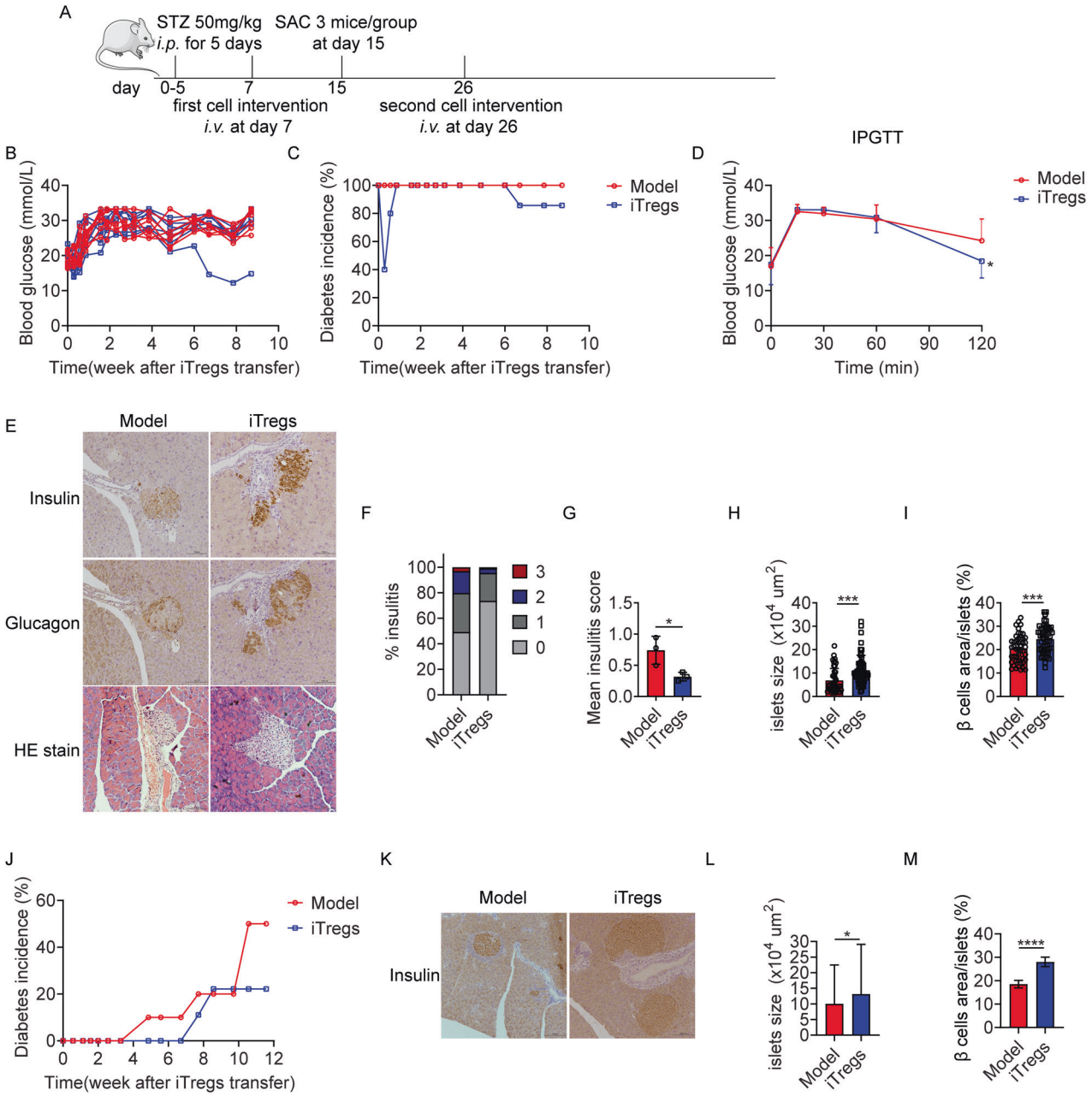

Fig. 6 iTregs improved β cell function in mice with established T1D. Diabetes was induced in C57BL/6 mice with STZ, and iTregs were injected after disease onset. **A** Schematic diagram for the therapeutic experiment. iTregs were injected into diabetic mice ($n = 10$) 7 days after STZ injection, and three mice with improved β cell function were sacrificed eight days after the cell intervention for analysis of the pancreas. A second injection of iTregs was performed 26 days after the STZ injection ($n = 7$), and blood glucose levels were monitored thereafter. **B** Nonfasting blood glucose levels are shown ($n = 7$–10). **C** Diabetes incidence is shown. **D** Results for an IPGTT performed one week after iTregs injection are shown. Two-tailed unpaired *t*-test; data are shown as the mean ± s.d. Three mice per group were sacrificed eight days after the first iTregs injection. Representative images of HE, insulin and glucagon staining (**E**). Statistical analysis of insulitis scores between the groups ($n = 3$). Two-tailed unpaired *t* test; data are shown as the mean ± s.d (**F**, **G**). All islets seen in three sections per pancreas were included in the analysis. Statistical analysis of islet area (**H**) and β cell area in relation to islet area (**I**). Two-tailed unpaired *t* test; data are shown as the mean ± s.d. iTregs were injected into 6-week-old ($n = 5$ for each group) and 10-week-old ($n = 5$ for each group) NOD mice. Week 0 was the day of iTregs injection, and blood glucose levels were monitored for 81 days. **J** Diabetes incidence in the two groups. **K** Representative image of insulin staining. All islets seen in three sections per pancreas were included in the analysis. Statistical analysis of islet area (**L**) and β cell area in relation to islet area (**M**). Two-tailed unpaired *t*-test; data are shown as the mean ± s.d. $^*P < 0.05$, $^{***}P < 0.001$, and $^{****}P < 0.0001$

function between the two groups 40 days after cell transfer. The differences in blood glucose levels at different time points during the IPGTT experiment and the AUC of the IPGTT did not reach statistical significance (Supplementary Fig. S8B, C). Insulin staining revealed that mice treated with iTregs retained a remarkably larger islet area and more insulin-producing pancreatic β cells (Fig. 6K–M and Supplementary Fig. S8D, E). In summary, these results indicated that iTregs could improve β cell function to a certain degree when transferred in the context of established T1D.

DISCUSSION

T1D patients have been shown to have defects in the frequency and/or function of Treg cells,[9–11] which are protective in animal and human T1D.[12–14] To date, the role of a more stable Treg population, iTregs, in T1D has seldom been studied. In this paper, we found that iTregs were stable, which is consistent with the findings in other papers,[15,19] as they maintained high levels of Foxp3 expression while seldom expressing proinflammatory cytokines, such as IL-17A and IFN-γ. These iTregs induced in vitro were protective in STZ-induced T1D. They could delay T1D onset and ameliorate disease severity, as shown by reduced blood glucose levels, decreased islet damage, and improved β cell morphology and function.

The T1D model established with multiple low-dose STZ injections is an extensively used T1D model. Regardless of a direct toxic effect, a subsequent autoimmune reaction has been demonstrated to lead to β cell apoptosis, which then induces infiltration of T cells into the islets, suggesting a role for immune imbalance in this model.[46] Therefore, it is not surprising that iTregs are functional in STZ-T1D since iTregs have a strong immunosuppressive function.

Although some previous studies have reported the therapeutic potential of iTregs in T1D,[25–27] the mechanism has not been thoroughly investigated, except for one paper that mentioned that iTregs might work by inhibiting Th1 cells via FasL-dependent cytotoxicity.[25] As T1D is widely recognized as an autoimmune disease and iTregs mainly function through immunosuppression, we further elucidated the mechanisms by which iTregs protect against T1D. Among proinflammatory T cell subsets, Tc1 cells are the population primarily suppressed by iTregs. As cytotoxic Tc1 cells accumulate with disease progression in prediabetic mice and patients newly diagnosed with type 1 diabetes, we concluded that prompt subversion of $CD8^+$ T cell effector function underlies the efficacy of iTregs therapy in preserving the function of islet β cells. The possible mechanisms could be attributed to decreased Tc1 cell proliferation, increased Tc1 cell apoptosis, reduced Tc1 cell infiltration and/or inhibited Tc1 cell differentiation. Our results showed that iTregs did not affect the proliferation or apoptosis of $CD8^+$ T cells in the spleen or lymph nodes in vivo but significantly suppressed Tc1 cell polarization in vitro. The elevated expression of CCR5, whose ligands are CCL3, CCL4, and CCL5, on Tc1 cells contributes to the preferential recruitment of Tc1 cells in target tissues.[8,47] Previous reports by Morlacchi et al. and others have demonstrated that Tregs can target dendritic cell-mediated proinflammatory chemokine (CCL3 and CCL4) production, thus mediating a decrease in the recruitment of target T cells.[48,49] Whether iTregs have the ability to decrease the migration of Tc1 cells to target tissues in T1D mice remains elusive and is worthy of further study in the near future.

Transforming growth factor-β is an important pleiotropic cytokine with potent immunoregulatory properties that has been reported to be crucial for iTregs-mediated suppressive function.[38,39] TGF-β can inhibit IFN-γ expression during Th1 cell development.[50] Moreover, a paper reported that TGF-β signals were critical for $CD4^+$ $CD25^+$ Treg cell-mediated regulation of autoreactive islet-specific cytotoxic T lymphocytes in a $CD8^+$ T cell-mediated model of T1D.[51] Unsurprisingly, we proved that the regulatory effect of iTregs on Tc1 cells was also dependent on TGF-β since blocking TGF-β signaling using an ALK5 inhibitor completely eliminated the suppression of IFN-γ production in $CD8^+$ T cells in vitro.

Follicular regulatory T cells can significantly suppress the activation of $CD8^+$ T cells in a manner dependent on IL-10 and probably TGF-β.[52] IL-10 has also been reported to be important for iTregs' immunomodulatory function.[38] However, in our study, we found that IL-10 signaling was dispensable for the suppressive function of iTregs during Tc1 cell polarization in vitro, since IFN-γ expression was not significantly changed when we added serial doses of an anti-IL-10 antibody to the culture system (data not shown). This difference could be explained by the different cell culture systems and different index parameters used.

Since studies have shown a requirement for mTOR activity in the maintenance of effector $CD8^+$ T cell differentiation and mTOR was reported to be a critical target of TGF-β in mouse and human NK cells leading to arrest of NK cell development and cytotoxic activity,[53,54] it is reasonable to conclude that iTregs suppress Tc1 cell differentiation through TGF-β-mediated mTOR inactivation. TCF1 deficiency resulted in increased IFN-γ production in $CD4^+$ T cells, while overexpression of TCF1 led to suppression of IFN-γ production.[55] Recent studies have shown that TCF1 suppresses effector $CD8^+$ T cell differentiation and function directly or indirectly via epigenetic modification of the IFN-γ enhancer and that the Tcf1 dose and protein stability are critical in suppressing IFN-γ production.[56] All of these papers support our findings that iTregs might inhibit Tc1 cells by maintaining high expression of the TCF1 protein. Our results showed that TGF-β was also required for this effect. One possible mechanism underlying the sustained expression of TCF1 mediated by TGF-β might be inhibiting the expression of the transcription factor signal transducer and activator of transcription (STAT) 4, since the inflammatory cytokine IL-12 used in the Tc1 cell polarization system can induce TCF1 downregulation via STAT4,[45] and TGF-β was reported to inhibit Th1 cell differentiation specifically through downregulation of STAT-4 expression.[57] Nevertheless, further experiments, especially with transgenic mice, are needed to provide direct evidence for how TGF-β inhibits mTOR activation and maintains TCF1 expression and define the relationship between mTOR and TCF1 signaling in Tc1 cells during diabetes.

Since iTregs showed such powerful protection against diabetes onset, we evaluated their role in established T1D. As the data revealed, iTregs decreased the blood glucose level and improved β cell function soon after cell transfer, but these effects lasted for only several days. iTregs mainly function through immune suppression, and after cell transfer, iTregs could significantly inhibit the autoimmune response in diabetic mice, which led to the decreased blood glucose levels and improved β cell function. However, the autoimmune response in early-onset diabetic mice might be so strong that the iTregs failed to persistently suppress it, which resulted in the blood glucose level rebounding. Increasing the iTregs cell number and frequency in products for cell transfer might help to solve this problem, which could be further tested. Surprisingly, one mouse achieved a normal blood glucose level approximately two months after iTregs injection. One explanation might be that iTregs have the ability to repair damaged tissue in addition to performing their immunosuppressive function. Previous papers have reported that Tregs can promote tissue repair through direct interactions with tissue progenitor cells or through interactions with supportive cells to create an appropriate stem cell niche for tissue repair,[58] and amphiregulin,[59] keratinocyte growth factor,[60] CCN3,[61] VEGFA,[62] Jag1,[63] and IL-10[64] play important roles in the process of tissue repair. In the near future, it would be of interest to determine whether iTregs have a regenerative role in T1D mice or other disease models.

In addition to the STZ-T1D model, NOD mice, which spontaneously develop diabetes, were also used to explore the therapeutic role of iTregs. Due to the limitation of the small sample size, we could see only a potential decrease in blood glucose levels and delay of diabetes onset. Strikingly, iTregs indeed maintained larger islet sizes and more functional β cells, which motivated us to optimize the dose and frequency of the cell intervention and use a larger number of NOD mice in the future to further clarify the therapeutic role of iTregs.

In conclusion, the current work demonstrated the therapeutic role of iTregs in autoimmune responses and β cell protection in the STZ-T1D model. The underlying mechanisms might be associated with a TGF-β-dependent reduction in IFN-γ expression

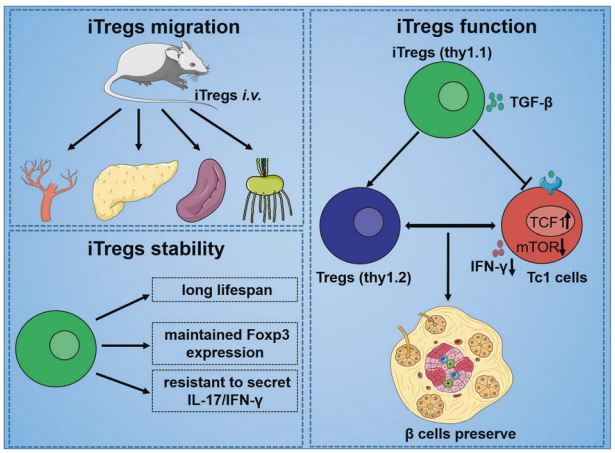

Fig. 7 Model of iTregs migration, stability and function in STZ-T1D mice. iTregs migrated to PBMCs, the pancreas, the spleen and the lymph nodes. iTregs survived for at least 30 days in STZ-T1D mice and were stable in vivo, as indicated by the maintained expression of Foxp3 and resistance to secretion of IL-17 and IFN-γ. iTregs could protect β cell function, possibly by upregulating Treg levels in recipient mice while inhibiting type 1 cytotoxic T cell (Tc1) function, thus rebalancing the Treg/Tc1 cell ratio in recipients. The effect of iTregs on Tc1 cells was dependent on TGF-β-mediated combinational action on mTOR and TCF1 signaling

in $CD8^+$ T cells. At the molecular level, the repression of mTOR activation and maintenance of high expression of the TCF1 protein by TGF-β could both be involved in the iTregs-mediated suppression of Tc1 cells (Fig. 7). Our work indicates a potential novel therapeutic strategy for delaying the occurrence and development of diabetes.

ACKNOWLEDGEMENTS

This work was supported by the National Key R&D Program of China (2017YFA0105803), the general program of the National Natural Science Foundation of China (81770826), the Science and Technology Plan Projects of Guangdong Province (2019B020227003), the Key Special Projects of Medical and Health of Guangzhou City (202007040003), and the 5010 Clinical Research Projects of Sun Yat-sen University (2015015). Y.M.C. designed the experiments and helped write the manuscript. L.Z. and X.M.H. performed most experiments and collected data. P.H.C. and J.L.D. participated in experiments during revision. L.Z., X.M.H., T.L., R.D.P. analyzed the data. Y.L., H.C.L., F.H., G.J.S., and C.C.X. contributed administrative, technical or material support. L.Z. and Y.L. wrote the manuscript. We thank Song Guo Zheng (Professor of Medicine, Department of Internal Medicine, Ohio State University College of Medicine) for sharing his wisdom with us during the course of this research and for providing comments that greatly improved the manuscript. We thank Julie Wang for providing technical support and helping us with the study design.

ADDITIONAL INFORMATION

The online version of this article (https://doi.org/10.1038/s41423-020-00623-2) contains supplementary material.

Competing interests: The authors have no competing interests that might be perceived as influencing the results and/or discussion in this paper. The authors declare no competing interests.

REFERENCES

1. Patterson, C. C. et al. Trends and cyclical variation in the incidence of childhood type 1 diabetes in 26 European centres in the 25 year period 1989-2013: a multicentre prospective registration study. *Diabetologia* **62**, 408–17. (2019).
2. Livingstone, S. J. et al. Estimated life expectancy in a Scottish cohort with type 1 diabetes, 2008-2010. *JAMA* **313**, 37–44 (2015).
3. Greenbaum, C. J. et al. Strength in numbers: opportunities for enhancing the development of effective treatments for type 1 diabetes—the TrialNet experience. *Diabetes* **67**, 1216–25. (2018).
4. Eizirik, D. L., Colli, M. L. & Ortis, F. The role of inflammation in insulitis and beta-cell loss in type 1 diabetes. *Nat. Rev. Endocrinol.* **5**, 219–26. (2009).
5. Willcox, A., Richardson, S. J., Bone, A. J., Foulis, A. K. & Morgan, N. G. Analysis of islet inflammation in human type 1 diabetes. *Clin. Exp. Immunol.* **155**, 173–81. (2009).
6. Coppieters, K. T. et al. Demonstration of islet-autoreactive CD8 T cells in insulitic lesions from recent onset and long-term type 1 diabetes patients. *J. Exp. Med.* **209**, 51–60 (2012).
7. Menart-Houtermans, B. et al. Leukocyte profiles differ between type 1 and type 2 diabetes and are associated with metabolic phenotypes: results from the German Diabetes Study (GDS). *Diabetes Care* **37**, 2326–33. (2014).
8. Vizler, C. et al. Relative diabetogenic properties of islet-specific Tc1 and Tc2 cells in immunocompetent hosts. *J. Immunol.* **165**, 6314–21. (2000).
9. Buckner, J. H. Mechanisms of impaired regulation by CD4(+)CD25(+)FOXP3(+) regulatory T cells in human autoimmune diseases. *Nat. Rev. Immunol.* **10**, 849–59. (2010).
10. Ferraro, A. et al. Expansion of Th17 cells and functional defects in T regulatory cells are key features of the pancreatic lymph nodes in patients with type 1 diabetes. *Diabetes* **60**, 2903–13. (2011).
11. Ryba-Stanislawowska, M., Skrzypkowska, M., Mysliwiec, M. & Mysliwska, J. Loss of the balance between CD4(+)Foxp3(+) regulatory T cells and CD4(+)IL17A (+) Th17 cells in patients with type 1 diabetes. *Hum. Immunol.* **74**, 701–707 (2013).
12. Lundsgaard, D., Holm, T. L., Hornum, L. & Markholst, H. In vivo control of diabetogenic T-cells by regulatory CD4+CD25+ T-cells expressing Foxp3. *Diabetes* **54**, 1040–1047 (2005).
13. Jaeckel, E., von Boehmer, H. & Manns, M. P. Antigen-specific FoxP3-transduced T-cells can control established type 1 diabetes. *Diabetes* **54**, 306–10. (2005).
14. Marek-Trzonkowska, N. et al. Administration of CD4+CD25highCD127- regulatory T cells preserves beta-cell function in type 1 diabetes in children. *Diabetes Care* **35**, 1817–20. (2012).
15. Horwitz, D. A., Zheng, S. G. & Gray, J. D. Natural and TGF-beta-induced Foxp3(+) CD4(+) CD25(+) regulatory T cells are not mirror images of each other. *Trends Immunol.* **29**, 429–35. (2008).
16. Zhou, X. et al. Cutting edge: all-trans retinoic acid sustains the stability and function of natural regulatory T cells in an inflammatory milieu. *J. Immunol.* **185**, 2675–2679 (2010).
17. Komatsu, N. et al. Pathogenic conversion of Foxp3+ T cells into TH17 cells in autoimmune arthritis. *Nat. Med.* **20**, 62–68 (2014).
18. Xu, W. et al. Adoptive transfer of induced-Treg cells effectively attenuates murine airway allergic inflammation. *Plos One* **7**, e40314 (2012).
19. Zheng, S. G., Wang, J. & Horwitz, D. A. Cutting edge: Foxp3+CD4+CD25+ regulatory T cells induced by IL-2 and TGF-beta are resistant to Th17 conversion by IL-6. *J. Immunol.* **180**, 7112–7116 (2008).
20. Xu, L., Kitani, A., Fuss, I. & Strober, W. Cutting edge: regulatory T cells induce CD4 +CD25-Foxp3- T cells or are self-induced to become Th17 cells in the absence of exogenous TGF-beta. *J. Immunol.* **178**, 6725–6729 (2007).
21. Lan, Q. et al. Induced Foxp3(+) regulatory T cells: a potential new weapon to treat autoimmune and inflammatory diseases? *J. Mol. Cell Biol.* **4**, 22–28 (2012).
22. Kong, N. et al. Induced T regulatory cells suppress osteoclastogenesis and bone erosion in collagen-induced arthritis better than natural T regulatory cells. *Ann. Rheum. Dis.* **71**, 1567–72. (2012).
23. Kong, N. et al. Antigen-specific transforming growth factor β-induced Treg cells, but not natural Treg cells, ameliorate autoimmune arthritis in mice by shifting the Th17/Treg cell balance from Th17 predominance to Treg cell predominance. *Arthritis Rheum.* **64**, 2548–58. (2012).
24. Selvaraj, R. K. & Geiger, T. L. Mitigation of experimental allergic encephalomyelitis by TGF-beta induced Foxp3+ regulatory T lymphocytes through the induction of anergy and infectious tolerance. *J. Immunol.* **180**, 2830–2838 (2008).
25. Weber, S. E. et al. Adaptive islet-specific regulatory CD4 T cells control autoimmune diabetes and mediate the disappearance of pathogenic Th1 cells in vivo. *J. Immunol.* **176**, 4730–4739 (2006).
26. Luo, X. et al. Dendritic cells with TGF-beta1 differentiate naive CD4+CD25- T cells into islet-protective Foxp3+ regulatory T cells. *Proc. Natl Acad. Sci. USA* **104**, 2821–2826 (2007).
27. Jones, C. B. et al. Regulatory T cells control diabetes without compromising acute anti-viral defense. *Clin. Immunol.* **153**, 298–307 (2014).
28. Elias, D. et al. Autoimmune diabetes induced by the beta-cell toxin STZ. Immunity to the 60-kDa heat shock protein and to insulin. *Diabetes* **43**, 992–998 (1994).
29. Kantwerk, G., Cobbold, S., Waldmann, H. & Kolb, H. L. 3T. 4 and Lyt-2 T cells are both involved in the generation of low-dose streptozotocin-induced diabetes in mice. *Clin. Exp. Immunol.* **70**, 585–592 (1987).

30. Nakamura, M., Nagafuchi, S., Yamaguchi, K. & Takaki, R. The role of thymic immunity and insulitis in the development of streptozocin-induced diabetes in mice. *Diabetes* **33**, 894–900 (1984).
31. Buschard, K. & Rygaard, J. T-lymphocytes transfer streptozotocin induced diabetes mellitus in mice. *Acta Pathol. Microbiol Scand. C* **86C**, 277–82. (1978).
32. Goyal, S. N. et al. Challenges and issues with streptozotocin-induced diabetes—a clinically relevant animal model to understand the diabetes pathogenesis and evaluate therapeutics. *Chem. Biol. Interact.* **244**, 49–63 (2016).
33. Shimokawa, C. et al. CD8(+) regulatory T cells are critical in prevention of autoimmune-mediated diabetes. *Nat. Commun.* **11**, 1922 (2020).
34. Müller, A., Schott-Ohly, P., Dohle, C. & Gleichmann, H. Differential regulation of Th1-type and Th2-type cytokine profiles in pancreatic islets of C57BL/6 and BALB/c mice by multiple low doses of streptozotocin. *Immunobiology* **205**, 35–50 (2002).
35. Kondo, S. et al. Suppression of insulitis and diabetes in B cell-deficient mice treated with streptozocin: B cells are essential for the TCR clonotype spreading of islet-infiltrating T cells. *Int Immunol.* **12**, 1075–83. (2000).
36. Cai, W. et al. All trans-retinoic acid protects against acute ischemic stroke by modulating neutrophil functions through STAT1 signaling. *J. Neuroinflamm.* **16**, e175 (2019).
37. Yadav, M. et al. Neuropilin-1 distinguishes natural and inducible regulatory T cells among regulatory T cell subsets in vivo. *J. Exp. Med.* **209**, 1713–1722 (2012). S1–19.
38. Zheng, S. G., Wang, J. H., Gray, J. D., Soucier, H. & Horwitz, D. A. Natural and induced CD4+CD25+ cells educate CD4+CD25- cells to develop suppressive activity: the role of IL-2, TGF-beta, and IL-10. *J. Immunol.* **172**, 5213–21. (2004).
39. Xu, A. et al. TGF-beta-induced regulatory T cells directly suppress B cell responses through a noncytotoxic mechanism. *J. Immunol.* **196**, 3631–41. (2016).
40. Araki, K. et al. mTOR regulates memory CD8 T-cell differentiation. *Nature* **460**, 108–12. (2009).
41. Rao, R. R., Li, Q., Odunsi, K. & Shrikant, P. A. The mTOR kinase determines effector versus memory CD8+ T cell fate by regulating the expression of transcription factors T-bet and Eomesodermin. *Immunity* **32**, 67–78 (2010).
42. Ito, D. et al. mTOR complex signaling through the SEMA4A–Plexin B2 axis is required for optimal activation and differentiation of CD8+T cells. *J. Immunol.* **195**, 934–43. (2015).
43. Yu, Q., Sharma, A. & Sen, J. M. TCF1 and β-catenin regulate T cell development and function. *Immunol. Res* **47**, 45–55 (2010).
44. Donnarumma, T. et al. Opposing development of cytotoxic and follicular helper CD4 T cells controlled by the TCF-1-Bcl6 nexus. *Cell Rep.* **17**, 1571–83. (2016).
45. Danilo, M., Chennupati, V., Silva, J. G., Siegert, S. & Held, W. Suppression of Tcf1 by inflammatory cytokines facilitates effector CD8 T cell differentiation. *Cell Rep.* **22**, 2107–17. (2018).
46. O'Brien, B. A., Harmon, B. V., Cameron, D. P. & Allan, D. J. Beta-cell apoptosis is responsible for the development of IDDM in the multiple low-dose streptozotocin model. *J. Pathol.* **178**, 176–81. (1996).
47. Cerwenka, A., Morgan, T. M., Harmsen, A. G. & Dutton, R. W. Migration kinetics and final destination of type 1 and type 2 CD8 effector cells predict protection against pulmonary virus infection. *J. Exp. Med.* **189**, 423–34. (1999).
48. Morlacchi, S. et al. Regulatory T cells target chemokine secretion by dendritic cells independently of their capacity to regulate T cell proliferation. *J. Immunol.* **186**, 6807–14. (2011).
49. Dal Secco, V. et al. Tunable chemokine production by antigen presenting dendritic cells in response to changes in regulatory T cell frequency in mouse reactive lymph nodes. *Plos One* **4**, e7696 (2009).
50. Lin, J. T., Martin, S. L., Xia, L. & Gorham, J. D. TGF-beta 1 uses distinct mechanisms to inhibit IFN-gamma expression in CD4+ T cells at priming and at recall: differential involvement of Stat4 and T-bet. *J. Immunol.* **174**, 5950–5958 (2005).
51. Green, E. A., Gorelik, L., McGregor, C. M., Tran, E. H. & Flavell, R. A. C. D. 4 CD25+ T regulatory cells control anti-islet CD8+ T cells through TGF-beta-TGF-beta receptor interactions in type 1 diabetes. *Proc. Natl Acad. Sci. USA* **100**, 10878–83. (2003).
52. Li, L., Ma, Y. & Xu, Y. Follicular regulatory T cells infiltrated the ovarian carcinoma and resulted in CD8 T cell dysfunction dependent on IL-10 pathway. *Int. Immunopharmacol.* **68**, 81–87 (2019).
53. Shirasaki, T. et al. Impaired interferon signaling in chronic hepatitis C patients with advanced fibrosis via the transforming growth factor beta signaling pathway. *Hepatology* **60**, 1519–30. (2014).
54. Viel, S. et al. TGF-beta inhibits the activation and functions of NK cells by repressing the mTOR pathway. *Sci. Signal.* **9**, a19 (2016).
55. Yu, Q. et al. T cell factor 1 initiates the T helper type 2 fate by inducing the transcription factor GATA-3 and repressing interferon-gamma. *Nat. Immunol.* **10**, 992–999 (2009).
56. Tiemessen, M. M. et al. T Cell factor 1 represses CD8+ effector T cell formation and function. *J. Immunol.* **193**, 5480–5487 (2014).
57. Das, J. et al. Transforming growth factor beta is dispensable for the molecular orchestration of Th17 cell differentiation. *J. Exp. Med.* **206**, 2407–16. (2009).
58. Fung, T. H. W., Yang, K. Y. & Lui, K. O. An emerging role of regulatory T-cells in cardiovascular repair and regeneration. *Theranostics* **10**, 8924–38. (2020).
59. Burzyn, D. et al. A special population of regulatory T cells potentiates muscle repair. *Cell* **155**, 1282–95. (2013).
60. Dial, C. F., Tune, M. K., Doerschuk, C. M. & Mock, J. R. Foxp3(+) regulatory T cell expression of keratinocyte growth factor enhances lung epithelial proliferation. *Am. J. Respir. Cell Mol. Biol.* **57**, 162–73. (2017).
61. Dombrowski, Y. et al. Regulatory T cells promote myelin regeneration in the central nervous system. *Nat. Neurosci.* **20**, 674–80. (2017).
62. Facciabene, A. et al. Tumour hypoxia promotes tolerance and angiogenesis via CCL28 and T(reg) cells. *Nature* **475**, 226–30. (2011).
63. Ali, N. et al. Regulatory T cells in skin facilitate epithelial stem cell differentiation. *Cell* **169**, 1119–29. (2017).
64. Sharir, R. et al. Regulatory T cells influence blood flow recovery in experimental hindlimb ischaemia in an IL-10-dependent manner. *Cardiovasc. Res.* **103**, 585–96. (2014).